

Threshold reduction in pierced microdisk lasers

S. A. Backes and J. R. A. Cleaver^{a)}

Microelectronics Research Centre, Cavendish Laboratory, Madingley Road, Cambridge CB3 0HE, United Kingdom

A. P. Heberle and J. J. Baumberg

Hitachi Cambridge Laboratory, Cavendish Laboratory, Madingley Road, Cambridge CB3 0HE, United Kingdom

K. Köhler

Fraunhofer-Institut für Angewandte Festkörperphysik, 79108 Freiburg, Germany

(Received 23 June 1998; accepted for publication 26 October 1998)

GaAs microdisk lasers with holes pierced through the disk surface are investigated for their threshold characteristics. Disks are fabricated with either a single hole or two diametrically opposite holes at various distances from the disk outer edge. Even though the disk area is reduced by only 1%, we find that the lasing threshold for a disk with one hole is reduced by up to 50% compared to a disk with no hole. We attribute this reduction to the perturbation of nonlasing modes, which decreases the amplification of spontaneous emission in these modes and makes more carriers available to contribute to lasing. © 1999 American Institute of Physics. [S0003-6951(99)00301-0]

Semiconductor microdisk lasers are of interest for micron-scale low-threshold laser devices. Their laser modes approximate whispering-gallery (WG) modes, for which the high reflectivity at the curved disk boundary gives low-threshold operation. The laser threshold is a function of the optical confinement, gain/absorption balance, scattering processes, and device dimensions. The optical confinement in these structures is high because of the large dielectric discontinuity between the disk and the surrounding air, while carrier absorption and scattering processes are difficult to modify. Threshold characteristics can be calculated,¹⁻³ and various research groups have sought to achieve low-threshold operation by shrinking the device dimensions to reduce spontaneous emission into nonlasing modes;⁴⁻⁶ the smallest microdisk laser reported having 1.6 μm diameter.⁵ Other groups have concentrated on optimizing the edge quality of their devices to improve the optical confinement, resulting in further reductions of the laser threshold.⁷

In this letter we present an approach for decreasing the threshold in a large semiconductor disk ($R \gg \lambda$) based on reducing the amplified spontaneous emission (ASE) into competing nonlasing modes. We achieve this reduction by removing material from the interior of the disk, which reduces the photon lifetimes for modes with field in this region. Since the ASE depends on the photon lifetimes of the corresponding modes, fewer carriers emit into these modes, making more carriers available to contribute to lasing. The introduction of one small hole, comprising approximately 1% of the disk area, can reduce the laser threshold by a factor of 2.

Figure 1 shows an electron micrograph of a typical microdisk structure with small holes etched through the top surface (Fig. 1). The disks contain four 10 nm GaAs quantum wells (QWs) separated by $\text{Al}_{0.28}\text{Ga}_{0.72}\text{As}$ barriers, and are defined by electron-beam lithography and reactive ion etching. The pedestals (500 nm $\text{Al}_{0.65}\text{Ga}_{0.35}\text{As}$) are created

by undercutting with a selective wet etch. Finally, the structures are passivated in ammonium sulphide and stabilized with a 30-nm-thick silicon nitride encapsulation.⁸ The disks have a diameter of 12.6 μm with 0.5 μm square holes. Disks have been fabricated with one hole, or two holes placed opposite each other, separated from the disk outer edge by 0.5, 1, 1.5, 2, or 2.5 μm . Devices were fabricated in square arrays with a 75 μm pitch. To increase the vertical collection efficiency of the edge emission, scattering structures comprising 15 μm wide mesas were placed 5 μm away from each row of disks, on the side of a hole.

The modes in a dielectric disk are solutions of the three-dimensional Maxwell equations. For disk thicknesses less than $\lambda/2\eta_{\text{eff}}$, where λ is the free-space wavelength and η_{eff} is the effective refractive index, the three-dimensional system can be approximated by a two-dimensional one described by the Helmholtz equation, $(\nabla^2 + 4\pi^2\eta_{\text{eff}}^2/\lambda^2)\psi=0$, which yields Bessel-function solutions for the radial field distribution: $\psi(r) \propto J_{m,n}[(2\pi\eta_{\text{eff}}/\lambda)r]$. Here, $J_{m,n}$ is the Bessel function of number m and order n .

^{a)}Electronic mail: jrac@hermes.cam.ac.uk

FIG. 1. Microdisk laser of radius 6.3 μm with two holes at a distance of 0.5 μm from the edge. In this scanning electron micrograph image, the electron beam penetrates the disk, showing the etched underlying pedestal.

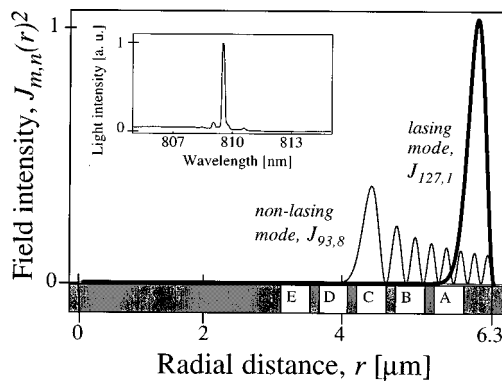


FIG. 2. Radial intensity distribution of the lasing first-order WG mode (thick line) and a nonlasing higher-order WG mode (thin line) for a $6.3 \mu\text{m}$ radius disk (Bessel-function number $m = 127$ and $m = 93$, respectively). The radial positions of the etched holes A, B, C, D, and E are, respectively, 0.5 , 1.0 , 1.5 , 2.0 , and $2.5 \mu\text{m}$ away from the disk edge. The field for the first-order mode has a full width at half maximum of 323 nm and its peak is situated 215 nm inside the disk edge. Inset: laser spectrum for a two-hole disk, representative of all microdisk devices measured.

The boundary condition for a first-order ($n = 1$) WG mode is the coincidence of the first node of the Bessel function with the disk edge; for a $6.3 \mu\text{m}$ radius disk radiating at 809 nm , $m = M_{\text{max}} = 127$. The intensity distribution of $J_{127,1}$ is plotted in Fig. 2, with that of a higher-order WG mode ($m = 93$, $n = 8$) for comparison. Here the lasing mode is assumed to be $J_{M_{\text{max}},1}$, whose field is concentrated just inside the disk edge and thus experiences the smallest losses. All modes with field further inside the disk are referred to as nonlasing modes ($J_{m < M_{\text{max}},n}$). Neglecting the finite field at the disk edge (needed for emission of the laser light from the curved boundary) and the effect of the pedestal, is expected to result in only small corrections to the description above. Superimposed on Fig. 2 are the hole positions. Since the holes break the circular symmetry, the Bessel-function picture above is useful only qualitatively for pierced disks.

The pierced microdisks were excited optically with a continuous-wave Ti:sapphire laser operating at 780 nm wavelength. The exciting light was focused through a long working-distance microscope objective ($\times 25$ magnification) to a spot $30 \mu\text{m}$ in diameter. The samples were mounted inside a microscope cryostat attached to an x - y - z stage, enabling excitation of different devices without changing the measurement conditions. All measurements were taken at a temperature of 10 K .

The inset in Fig. 2 shows a typical emission spectrum for a microdisk laser with two holes. All disks exhibited identical spectral features with a sharp laser line at 809.1 nm superimposed on the broad QW luminescence. The subsidiary peaks are associated with higher-order WG modes ($n \geq 2$), rather than the neighboring first-order WG modes ($n = 1$, $m = M_{\text{max}} \pm 1$), which would be spectrally separated by -6.0 and $+6.1 \text{ nm}$, respectively (relative to a gain width of 12 nm).

Emission measurements were made on the different one-hole and two-hole disks and compared to disks without holes (Fig. 3). Threshold determination in microcavity lasers is difficult due to their nonlinear lasing characteristics.⁹ For the purposes of this work, we defined the laser threshold by the spectrum in which the first laser peak appeared. This as-

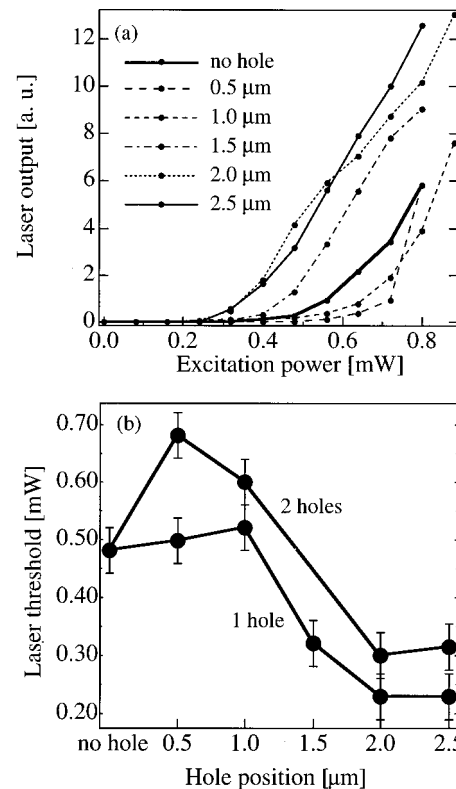


FIG. 3. (a) Laser emission dependence on pump power for disks with one hole for different edge-to-hole spacings. The excitation power corresponds to the power incident on the disk. (b) Variation in the threshold for the one-hole and two-hole disks.

sumes the laser light is collected at the onset of lasing. This method does not yield absolute threshold values but allows comparison of the lasing characteristics of these devices. The threshold values are of the same order as those given in the literature; e.g., $194 \mu\text{W}$ for a $5\text{-}\mu\text{m}$ -diam GaAs microdisk at 80 K .¹⁰

Threshold characteristics for the one-hole and two-hole disks are plotted in Fig. 3(b). The thresholds for the disks without holes are the same in both arrays, implying they were fabricated consistently. Compared to the disks with no holes, both the one-hole and the two-hole disks show threshold increases for the outer two-hole positions (0.5 and $1 \mu\text{m}$) and threshold reductions for the inner two-hole positions (2 and $2.5 \mu\text{m}$). The thresholds are lower for the one-hole disks compared to two-hole disks.

To interpret the data, we consider loss and gain contributions to the photoluminescence, to the laser field, and to the excited carrier distributions. Photoluminescence is affected in two ways. First, the etched hole can scatter non-guided spontaneously emitted light into all cavity modes, including the lasing mode. This pumping mechanism would affect the lasing mode and nonlasing modes equally, and not change the threshold. Second, the hole can influence the coupling of the photoluminescence to the pedestal, which is etched more for increasing edge-hole separations (as seen through the disk in Fig. 1). In the region of the disk above the pedestal, vertical confinement is precluded; light generated there is lost into the pedestal and cannot contribute to nonlasing modes. A smaller pedestal (larger undercut) will increase the photon lifetimes for nonlasing modes, causing more carriers to be lost through ASE to such modes. This

effect would increase the threshold for disks with smaller pedestals (greater hole/edge separations), which is not seen in the data, suggesting that this effect is not dominant.

The laser field can be affected by the hole in two ways. First, any additional decoupling of the laser mode and the pedestal is expected to be negligible, since the pedestal is already several wavelengths away from the laser mode even without the additional undercut due to the hole. Second, the laser mode intersects the hole for small hole/edge spacings, causing scattering of the laser light, thus reducing its photon lifetime and contributing to the threshold increase.

The excited carriers are likely to be affected by the holes in two ways. First, the holes introduce nonradiative recombination traps (GaAs surface states), locally reducing the probability of radiative recombination despite the sulphide passivation which is effective in reducing surface states. Given a carrier diffusion length of several micrometers, for small laser mode/hole separations excited carriers will be lost to these nonradiative traps, increasing the threshold. Such trapping should be stronger if there are more holes and this can be seen in Fig. 3(b) for hole positions $\leq 1 \mu\text{m}$ from the disk edge. For hole spacings $> 1 \mu\text{m}$, the surface states reduce radiative recombination into nonlasing modes, thus contributing to threshold reduction.

The second effect of the holes on the excited carriers is to increase the fraction of the ASE that is coupled into the laser mode, as a result of modifying the spatially overlapping but nonlasing resonator modes. For circularly symmetric disks, without holes, small variations in area will produce only minimal changes in the *relative* photon lifetimes between different cavity modes. However, if a small hole is introduced, it acts as a defect to perturb the modes which overlap the hole and reduces their photon lifetimes, while other modes are essentially unaffected. In this case, it is useful to define an amplified spontaneous emission factor, ζ , as the ratio of ASE into the lasing mode and nonlasing modes;

$$\zeta \equiv \frac{\text{ASE}_{\text{into lasing}}}{\text{ASE}_{\text{into nonlasing}}} \\ \equiv \frac{\int_0^R \{|A_{M_{\text{max},1}}(r)|^2 |A_{M_{\text{max},1}}(r)|^2 \tau_{M_{\text{max},1}}\} r dr}{\int_0^R \{\sum_{m,n}^{\neq 127,1} (|A_{m,n}(r)|^2 |A_{M_{\text{max},1}}(r)|^2) \tau_{m,n}\} r dr}.$$

Here the ASE into a mode is proportional to the product of the integrated modal intensity distribution and the photon lifetime, assuming a uniform carrier density excited across the QWs. The $A_{m,n}$ are the mode solutions which have wavelengths within the gain spectrum, r is the radial disk coordinate, R is the disk radius, $\tau_{m,n}$ is the modal photon lifetime, and $\int_0^R |A_{m,n}(r)|^2 dr$ have been normalized in area to each other. The product of the lasing and nonlasing fields in the denominator ensures that only nonlasing modes spatially overlapping the lasing mode are used. Although the overlap of an individual nonlasing mode with the lasing mode is small, the summation over all nonlasing modes makes the denominator significant. In a circularly symmetric cavity $A_{m,n} = J_{m,n}$. Changing the resonator geometry away from circular symmetry decreases the photon lifetimes of those modes whose trajectories are now asymmetric. The full calculation thus requires solving for the resonator modes in a three-dimensional asymmetrical cavity.

In the case of the pierced microdisk laser, the symmetry of the lasing mode is preserved, so $\tau_{M_{\text{max},1}}$ is constant, while certain nonlasing modes are severely attenuated due to their overlap with the holes. This leads to a favorably higher ζ compared to the no-hole case. The hole interrupts the optical path of all WG modes whose fields overlap the hole (e.g., $J_{93,8}$ with holes A, B, or C in Fig. 2) and replaces them with less confined and highly asymmetrical modes. These perturbed modes will pass through the pedestal region (where vertical confinement is not possible) or strike a hole/air or disk-edge/air boundary at an angle less than the critical angle and be strongly attenuated. The hole thus increases the loss of these perturbed nonlasing modes, substantially reducing their photon lifetimes compared to the previous nonlasing WG modes. Since the light in these modes also intersects the laser field located close to the periphery, the hole reduces the number of excited carriers that are lost through ASE to these nonlasing modes, increasing the ASE factor of the pierced disk. Placing a hole as close as possible to the disk periphery without directly interfering with the lasing mode itself, will degrade the greatest number of nonlasing modes and minimize the threshold; as the hole is moved further inwards, more modes will turn into WG modes with a higher photon lifetime and the threshold will again increase to its ‘‘no-hole’’ value. We consider this to be the dominant mechanism for reducing the laser threshold in the pierced microdisks.

In conclusion, we have demonstrated how engineering differences between the photon lifetimes of lasing and nonlasing optical modes in microdisk resonators produce significant changes in the lasing threshold. An increase in threshold for disks with holes placed close to the edge of the disk is due to the scattering of the laser light by the holes and the absorption and trapping of excited carriers by surface states around the holes. The strong reduction in laser threshold for holes spaced $> 1 \mu\text{m}$ from the disk periphery is attributed to the reduction of the ASE into nonlasing modes, as this makes more carriers available for emission into the laser mode. Thus, improvements in performance of mesoscale lasers result from optimizing the *symmetry* of the different optical modes, as well as reducing their volume.

The authors would like to thank J. Allam for fruitful discussions and suggestions.

¹R. E. Slusher, A. F. J. Levi, U. Mohideen, S. L. McCall, S. J. Pearton, and R. A. Logan, Appl. Phys. Lett. **63**, 1310 (1993).

²M. K. Chin, D. Y. Chu, and S. Ho, J. Appl. Phys. **75**, 3302 (1994).

³B. Zhang, R. Wang, X. Ding, L. Dai, and S. Wang, Solid State Commun. **91**, 699 (1994).

⁴A. F. J. Levi, S. L. McCall, S. J. Pearton, and R. A. Logan, Electron. Lett. **29**, 1666 (1993).

⁵T. Baba, M. Fujita, A. Sakai, M. Kihara, and R. Watanabe, IEEE Photonics Technol. Lett. **9**, 878 (1997).

⁶S. A. Backes, A. P. Heberle, J. R. A. Cleaver, and K. Köhler, Phys. Status Solidi B **204**, 581 (1997).

⁷S. Ando, N. Kobayashi, and H. Ando, Jpn. J. Appl. Phys., Part 2 **34**, L4 (1995).

⁸W. S. Hobson, U. Mohideen, S. J. Pearton, R. E. Slusher, and F. Ren, Electron. Lett. **29**, 2199 (1993).

⁹R. E. Slusher and U. Mohideen, in *Optical Processes in Microcavities*, edited by R. C. Chang and A. J. Campillo (World Scientific, Singapore, 1995), Vol. 3.

¹⁰U. Mohideen, W. S. Hobson, S. J. Pearton, F. Ren, and R. E. Slusher, Appl. Phys. Lett. **64**, 1911 (1994).